

Published in final edited form as:

Agric For Meteorol. 2017 May 1; 237-238: 135–142. doi:10.1016/j.agrformet.2017.02.012.

Revisiting the choice of the driving temperature for eddy covariance CO₂ flux partitioning

Georg Wohlfahrt¹ and Marta Galvagno²

¹Institute of Ecology, University of Innsbruck, Innsbruck, AUSTRIA

²Environmental Protection Agency of Aosta Valley, ARPA VdA, Climate Change Unit, Aosta, ITALY

Abstract

So-called CO₂ flux partitioning algorithms are widely used to partition the net ecosystem CO₂ exchange into the two component fluxes, gross primary productivity and ecosystem respiration. Common CO₂ flux partitioning algorithms conceptualize ecosystem respiration to originate from a single source, requiring the choice of a corresponding driving temperature. Using a conceptual dual-source respiration model, consisting of an above- and a below-ground respiration source each driven by a corresponding temperature, we demonstrate that the typical phase shift between air and soil temperature gives rise to a hysteresis relationship between ecosystem respiration and temperature. The hysteresis proceeds in a clockwise fashion if soil temperature is used to drive ecosystem respiration, while a counter-clockwise response is observed when ecosystem respiration is related to air temperature. As a consequence, nighttime ecosystem respiration is smaller than daytime ecosystem respiration when referenced to soil temperature, while the reverse is true for air temperature. We confirm these qualitative modelling results using measurements of day and night ecosystem respiration made with opaque chambers in a short-statured mountain grassland. Inferring daytime from nighttime ecosystem respiration or *vice versa*, as attempted by CO₂ flux partitioning algorithms, using a single-source respiration model is thus an oversimplification resulting in biased estimates of ecosystem respiration. We discuss the likely magnitude of the bias, options for minimizing it and conclude by emphasizing that the systematic uncertainty of gross primary productivity and ecosystem respiration inferred through CO₂ flux partitioning needs to be better quantified and reported.

Keywords

gross primary productivity; ecosystem respiration; temperature; hysteresis; chamber; model

1 Introduction

Gross primary productivity (GPP; for a recent discussion on the definition of this term see Wohlfahrt and Gu, 2015) and ecosystem respiration (R_{eco}) are key concepts and terms in carbon cycle science (Chapin et al., 2006) and their magnitude determines the sign of the net

ecosystem CO₂ exchange, i.e. $NEE = GPP + R_{eco}$ (here and in the following we employ a sign convention according to which negative fluxes represent a net uptake of CO₂ by the underlying surface). Since GPP and R_{eco} mask each other in the NEE during daytime conditions, it is difficult, or even impossible, to directly quantify GPP and daily sums of R_{eco} and thus various methods, with quite different theoretical backgrounds, have emerged to indirectly disentangle GPP and R_{eco} : Partitioning based on (i) flux variance similarity theory (Scanlon and Sahu, 2008; Sulman et al., 2016), (ii) the isotopes of CO₂ (e.g. Bowling et al., 2001; Ogée et al., 2003; Wehr and Saleska, 2015), (iii) carbonyl sulfide (COS) exchange (e.g. Asaf et al., 2013; Commene et al., 2015), (iv) sun-induced fluorescence (SIF; e.g. Parazoo et al., 2014) and (v) the photo-chemical reflectance index (PRI; Hilker et al., 2014). The most widely applied method, however, are the so-called CO₂ flux partitioning algorithms (Lasslop et al., 2010; Reichstein et al., 2005), which within the FLUXNET project are applied in a consistent fashion globally at +500 sites (e.g. Papale et al., 2006; Tramontana et al., 2016).

CO₂ flux partitioning algorithms exploit, in one way or the other, the contrasting sign of nighttime (positive – net CO₂ release) and daytime (negative – net CO₂ uptake) NEE. The nighttime approach put forward by Reichstein et al. (2005) uses nighttime NEE measurements to parametrise a temperature-dependent model of R_{eco} . GPP is then inferred by extrapolating R_{eco} to daytime temperatures and by subtracting the latter term from NEE. The daytime approach by Lasslop et al. (2010) uses nighttime NEE measurements to parameterise the temperature sensitivity of R_{eco} , but then uses a light- and temperature-driven model to infer both GPP and R_{eco} from daytime data only.

While being simple and appealing in principle, CO₂ flux partitioning approaches have not escaped criticism. Methodological problems discussed are related to uncertainties associated with nighttime eddy covariance flux estimates (e.g. Aubinet, 2008; Speckman et al., 2015) and approaches of minimising these (e.g. Gu et al., 2005), different day and nighttime flux footprints and associated bias in R_{eco} (Wehr and Saleska, 2015) and possible artificial correlations between inferred GPP and R_{eco} (e.g. Baldocchi et al., 2015; Vickers et al., 2009). From a more process-oriented perspective, issues which have been discussed include short- *versus* longer-term temperature sensitivities of R_{eco} (Reichstein et al., 2005), the overestimation of R_{eco} during daytime conditions due to leaf mitochondrial respiration being lower in the light compared to darkness (Heskel et al., 2013; Wehr et al., 2016; Wohlfahrt et al., 2005b) and temperature-independent diurnal variations in ecosystem respiration components (e.g. Bahn et al., 2009).

Another issue, first addressed in a synthetic fashion by Lasslop et al. (2012), is related to the fact that both CO₂ flux partitioning algorithms conceptualise R_{eco} to result from a single source, requiring a corresponding driving temperature being chosen. While Lasslop et al. (2012) showed that differences in the correlations between various driving temperatures and nighttime NEE were minor, the authors also found that the choice of the driving temperature affected inferred GPP and R_{eco} estimates and that the time lag between air and soil temperature was the best indicator for these differences.

The main objective of the present paper is to revisit the effects related to the choice of the driving temperature on inferred GPP and R_{eco} . In particular we aim to (i) clarify the consequences of the phase shift between air and soil temperature using a simple dual-source model of ecosystem respiration, (ii) confirm the qualitative model predictions with day and night R_{eco} measurements from a mountain grassland made with opaque chambers, and (iii) discuss the implications of our findings for eddy covariance CO_2 flux partitioning.

2 Material and methods

Conceptual dual-source ecosystem respiration model

In order to analyse how differences in phase and amplitude of above- and below-ground temperature and differences in the associated respiration components affect the extrapolation of nighttime R_{eco} to daytime conditions (and *vice versa*) we used a simple conceptual model representing R_{eco} as the sum of an above- (R_{ag}) and below-ground (R_{bg}) respiration component, driven by the two corresponding temperatures (Wohlfahrt et al., 2005a):

$$R_{eco} = R_{ag} + R_{bg} \quad \text{Eq. (1)}$$

$$R_x = R_x @ T_{ref} e^{E_{o-x} (T_x - T_{ref})} \quad \text{Eq. (2)}$$

Here $R_x @ T_{ref}$ refers to the above-ground (R_{ag}) or below-ground (R_{bg}) respiration ($\mu\text{mol m}^{-2} \text{s}^{-1}$) at the reference temperature ($T_{ref} = 283.15 \text{ K}$), E_{o-x} to the temperature sensitivity (K^{-1}) and T_x either to air (T_a) or soil temperature (T_s) (K).

The diurnal course of above- and below-ground temperature was simulated according to Campbell and Norman (1998) using a sinusoidal model:

$$T = T_{avg} + A_o e^{-z/D} \sin[\pi/12 (t - t_o) - z/d], \quad \text{Eq. (3)}$$

where T_{avg} is the average daily temperature (K), A_o the daily temperature amplitude (K), t_o a phase-shift parameter ($t_o = 8$), z the soil depth (m), D the soil damping depth (m) and t represents time (hours). In order to simulate the temperature of the above-ground respiration component, the soil depth (z) was set to zero.

Study site

Direct measurements of nighttime and daytime dark ecosystem respiration were conducted at the FLUXNET site Torgnon (IT-Tor), a subalpine grassland located in the northwestern Italian Alps at 2160 m asl ($45^\circ 50'40'' \text{ N}$, $7^\circ 34'41'' \text{ E}$). The mean annual temperature is 3.1°C and annual precipitation 880 mm. The site is typically covered by a continuous snow cover from the end of October to late May. Vegetation is mainly composed by matgrass (*Nardus stricta*) with other graminoids and forbs as co-dominant species (e.g. *Arnica montana*, *Trifolium alpinum* and *Carex sempervirens*) and the soil was classified as

Cambisol (FAO). The peak value of leaf area index and canopy height is on average $2.2 \text{ m}^2 \text{ m}^{-2}$ and 20 cm, respectively. Additional information on the study site can be found in Galvagno et al. (2013).

Ecosystem respiration chamber measurements, data processing and analysis

The low stature of the vegetation allowed direct measurements of ecosystem respiration without the need for upscaling different respiration components. Chamber measurements were conducted from mid-June to mid-October 2010, i.e. during most of the snow-free period, with four automated opaque CO_2 flux chambers (model 8100-104, LI-COR, USA) connected to a LI-8100/8150 multiplexer system (LI-COR, USA). The four chambers measured consecutively with an observation length of 120 s and a deadband (the time interval before steady mixing is established) of 30 s. A delay time and purging period was also set between two sequential measurements to avoid contamination between chambers. Each chamber was sampled twice in a measurement cycle and the resulting fluxes were aggregated to half-hourly values. CO_2 fluxes were calculated with the manufacturer software as the time rate of change of CO_2 mixing ratio in the measurement chamber. Due to high and low turbulent mixing during day and night respectively, post-field adjustments of the deadband duration were applied to optimise the reliability of flux calculations (Brændholt et al., 2016).

Basic meteorological parameters were regularly measured at the study site. Air temperature was measured with a Pt1000 thermometer (HMP45, Vaisala, Finland) at 1.5 m above the ground and soil temperature with thermistors (Therm107, Campbell Scientific, USA) installed at different depths below ground (0.02, 0.10, 0.25 and 0.35 m). An infrared radiometer sensor (SI111, Apogee Instruments, USA) was installed to infer surface temperature.

Because measurements were made with opaque chambers, i.e. in darkness also during daytime, our daytime R_{eco} estimates do not include the reduction in leaf mitochondrial respiration in light (Heskel et al., 2013) and thus allow to directly compare nighttime with daytime R_{eco} without the associated complications (Wohlfahrt et al., 2005b; Wohlfahrt and Gu, 2015). This was confirmed experimentally by comparing measurements of chambers that had been dark-adapted for longer periods (up to one hour) with normally operating chambers (data not shown).

Night and daytime data were distinguished based on a threshold of calculated (after Ham, 2005) potential incident radiation of 20 W m^{-2} . The following analyses were carried out both with air temperature and the average soil temperature at 0.02 and 0.1 m soil depth. Preliminary analysis with the radiometrically inferred surface temperature and soil temperatures at 0.02 and 0.1 m depth showed that the results obtained with the two chosen driving temperatures were quantitatively and qualitatively representative (data not shown).

In order to quantify differences between night and daytime R_{eco} we followed two approaches: First, we categorized night and daytime data of the same day into one degree (separately for air and soil temperature) bins and statistically compared night and daytime R_{eco} in bins with more than three data points each by means of a paired Wilcoxon-Mann-

Whitney test at the $p < 0.05$ probability level. Second, we fitted a linearized version of Eq. (2), i.e.

$$\log(R_{eco}) = \log(R_{eco}@T_{ref}) + E_o(T_x - T_{ref}), \quad \text{Eq. (4)}$$

separately to night and daytime log-transformed R_{eco} (after confirming the assumption of normality and homoscedasticity through normality- and QQ-plots) and compared the resulting slopes and y -intercepts using a paired t -test at the $p < 0.05$ probability level. This analysis was conducted both with all data pooled, as well as with 5-day overlapping 15-day blocks of data. The regression analysis was also repeated with the Lloyd and Taylor (1994) model, which however yielded qualitatively and quantitatively similar results (data not shown).

3 Results and Discussion

Conceptual modelling analysis

During the diurnal cycle, air temperature leads soil temperature, which, with increasing soil depth, reaches progressively lower minima and maxima at progressively later times compared to air temperature (Fig. 1b) (Campbell and Norman, 1998). In the context of our temperature model (Eq. 3), the maximal and minimal air temperatures, $T_{avg} \pm A_0$, are reached at $t_0 \pm 6$ hours, maximal and minimal soil temperatures, $T_{avg} \pm A_0 \exp(-z/D)$, at $(12/\pi) * (z/D) + t_0 \pm 6$ hours (Fig. 1b). In the model, soil and above-ground respiration strictly follow the diurnal course of the respective driving temperatures (Fig. 1a). The diurnal course of R_{eco} , in contrast, reflects the additive contributions of both below- and above-ground respiration (Eq. 1) and reaches minima/maxima after that of air and before that of soil temperature (Fig. 1a).

As a consequence, R_{eco} is out of phase both with soil and air temperature, which in turn gives rise to hysteresis, if R_{eco} is plotted as a function of either soil (Fig. 1c) or air (Fig. 1d) temperature. For soil temperature, the hysteresis proceeds in a clockwise fashion, with higher R_{eco} during the warming phase, which is due to the leading air temperature driving a higher above-ground respiration contribution compared to the cooling phase (Fig. 1c). Conversely, the hysteresis proceeds in a counter-clockwise fashion for air temperature with higher R_{eco} during the cooling phase, which is due to the lag in soil temperature and thus a comparatively higher soil respiration contribution after the air temperature maximum has been reached (Fig. 1d).

Since nighttime overlaps with parts of the cooling phase of both soil and air temperature, R_{eco} is thus lower and higher, respectively, for the same temperature during nighttime compared to daytime (Figs. 1c d). Nighttime flux partitioning (Reichstein et al., 2005) thus underestimates daytime R_{eco} if soil temperature is used to parameterise nighttime R_{eco} and the reverse is true if air temperature is used (Figs. 1c d). Our analysis is thus consistent with the results of Lasslop et al. (2012), who inferred a larger R_{eco} based on air temperature. For the daytime flux partitioning approach (Lasslop et al., 2010), the same reasoning, but with reverse signs, applies (nighttime R_{eco} is overestimated based on soil temperature and

underestimated based on air temperature), however additional complications arise because the temperature sensitivity is taken from the nighttime data.

The magnitude of the over- and underestimation depends on the phase shift between soil and air temperature, the magnitude of soil and above-ground respiration, their temperature sensitivities and night length. Most naturally, the bias is minimal in situations when most of ecosystem respiration originates from one source only (e.g. below-ground) and the corresponding driving (e.g. soil) temperature is used to parameterise nighttime ecosystem respiration. The bias is thus likely to differ between sites characterised by differing soil to ecosystem respiration ratios (e.g. Janssens et al., 2001) and vary seasonally at a given site (e.g. Davidson et al., 2006). Dampening and phase shift of soil as opposed to air temperature in the model (Eq. 3) is determined by the ratio of the soil (z) to the damping depth (D). The latter amounts to around 0.1 m for moist mineral soils and 0.03-0.06 m for drier mineral or organic soils (Campbell and Norman, 1998). Dampening and phase shift at a given site/depth are thus likely to vary seasonally with soil moisture. The amplitude of soil temperature is reduced by $\exp(-z/D)$ compared to air temperature and the phase shifted by $(12/\pi)*(z/D)$. Lasslop et al. (2012) found a median lag time of around 2 hours at FLUXNET sites, which corresponds to approximately $z/D=0.52$ and a dampening of the soil temperature amplitude by a factor of 0.59. For $z/D \Rightarrow 0$, both air and soil temperature are similarly good predictors for daytime R_{eco} . As z/D increases, hysteresis develops and both soil and air temperature result in biased predictions of daytime R_{eco} , as discussed above. At greater soil depths, as soil temperature eventually becomes invariable during the diurnal cycle, the predictive power of air temperature increases again due to the soil contribution approaching a constant. For $z/D = 0.52$ our calculations suggest a bias of 10-20 %.

The length of the nighttime period further complicates matters, as it determines which part of the hysteresis loop is used in the regression and thus influences respiration at the reference temperature, the temperature sensitivity and the explained variance. At reasonably small values of z/D , the slopes of the warming and cooling phases are usually fairly similar (Fig. 1a). In order to avoid a bias in the temperature sensitivity, it is important to avoid including periods immediately after the maximum/before the minimum temperature (the turning points of the hysteresis loops; Fig. 1a), into the regression. This recommendation may interfere with the current practise of filtering nighttime NEE eddy covariance measurements for friction velocity (Gu et al., 2005) or early evening periods (van Gorsel et al., 2008; van Gorsel et al., 2007).

Experimental confirmation of conceptual modelling results

The major finding of the previous modelling analysis is that due to the hysteresis relationship between temperature and R_{eco} , a single-source respiration model infers nighttime R_{eco} to be smaller than daytime R_{eco} at the same soil temperature and *vice versa* for air temperature.

The hysteresis relationship demonstrated by means of the conceptual model is also evident in the measured data, in particular when R_{eco} is plotted as a function of air temperature (Fig. 2). Further confirmation of the conceptual model is presented in Figure 3, which shows the differences between measured nighttime and daytime R_{eco} at the same temperature (within

one degree bins). Among the temperature bins that resulted in significant differences (closed symbols in Fig. 3), nighttime R_{eco} was smaller than daytime R_{eco} in 81 % of all cases when soil temperature was used and the reverse was found in 87 % of all cases when air temperature was used. Heinemeyer et al. (2013), using the same chamber system with sown *Lolium perenne* L. mesocosms, also found nighttime R_{eco} to exceed daytime R_{eco} when expressed as a function of (chamber) air temperature, however speculated this phenomenon to reflect physiological inhibition of daytime R_{eco} . As hypothesised above, the difference between daytime and nighttime R_{eco} exhibited clear seasonality (Fig. 3), indicating, possibly phenologically driven, changes in the contribution of above- and below-ground respiration to R_{eco} .

Figure 4 shows the results of calibrating Eq. (4) with measured daytime and nighttime R_{eco} on a seasonal basis. Inferred R_{eco} at the reference temperature was significantly (indicated by closed symbols) lower during daytime compared to nighttime in 87 % of all cases when air temperature was used as a reference temperature. Conversely, R_{eco} at the reference temperature was significantly higher during daytime compared to nighttime in 61 % of all cases when soil temperature was used. The temperature sensitivity parameter (E_o , Eq. 4), tended to be anti-correlated with $R_{eco}@T_{ref}$ (i.e. a higher $R_{eco}@T_{ref}$ during nighttime going along with a higher E_o during daytime), suggesting these not to be independent. Differences in E_o between day and night were however less consistent compared to $R_{eco}@T_{ref}$. The coefficient of determination (R^2) and the root mean squared error (RMSE) were generally higher and lower, respectively, during daytime independent of whether soil or air temperature was used.

Implications for eddy covariance CO₂ flux partitioning

Given that our experimental data substantiate the insights from the conceptual model, that is that the hysteresis response of R_{eco} to temperature causes biased estimates if extrapolated between day and night conditions, the question arises how this problem can be avoided or at least minimized in the context of eddy covariance CO₂ flux partitioning. Lasslop et al. (2012) suggested exploring weighted average temperatures between soil and air temperatures and selecting the driving temperature based on the fraction of explained variance in nighttime NEE. As shown in Figure 5, the variability of nighttime R^2 was small between air ($R^2 = 0.66$) and soil ($R^2 = 0.61$) temperature and peaked at a weight of 0.54, i.e. close to the arithmetic average of both driving temperatures. In contrast to eddy covariance CO₂ flux partitioning applications, our data allow assessing the skill by which daytime R_{eco} can be estimated from a temperature weighted between air and soil temperature. As shown in Figure 5, choosing the weight which maximised the R^2 , did not minimize the root mean squared error (RMSE) and the mean error (ME) between simulated and measured daytime R_{eco} , which were minimised at larger weights of 0.84 and 0.92, respectively. This again is due to the phase shift between air and soil temperature and the resulting hysteresis between either temperature and R_{eco} and cautions against determining the weight by maximising the R^2 of nighttime data.

The qualitative simulations with the conceptual model (Fig. 1) suggest that instead of averaging the driving temperature, averaging the output obtained with soil and air

temperature, might be an option to reduce the bias, an approach which would also be applicable to eddy covariance CO₂ flux partitioning. As shown in Figure 6 and Table 1 for a scenario within which daytime R_{eco} was predicted based on nighttime R_{eco} , this approach yielded the highest modelling efficiency (MEF) and minimized the RMSE, not however the ME, which was smallest when soil temperature was used as the driving temperature.

4 Conclusions and Recommendations

Based on simulations with a conceptual dual-source ecosystem respiration model, we have conclusively shown that the phase shift between the air and soil temperatures driving, respectively, above-ground and below-ground respiration, causes a hysteresis in the response of R_{eco} to each of these driving temperatures (Fig. 1). As a consequence, estimated nighttime R_{eco} is smaller or larger compared to daytime R_{eco} , depending on the choice of the driving temperature. Even though R_{eco} under real-world conditions is composed by a multitude of respiration sources with differing driving temperatures, we were able to confirm these qualitative modelling results with experimental measurements of R_{eco} during day and night using opaque chambers in a mountain grassland ecosystem (Figs. 2-4).

The two most widely used CO₂ flux partitioning algorithms (Lasslop et al., 2010; Reichstein et al., 2005) conceptualise R_{eco} to originate from a single source and thus need to choose a corresponding driving temperature. The main conclusion from this paper is that this is an oversimplification resulting in biased R_{eco} estimates.

The bias is predicted to be largest for ecosystems whose below- and above-ground respiration sources contribute approximately equally to R_{eco} and when the two driving temperatures exhibit large phase shifts. It is thus likely, that available GPP and R_{eco} estimates for forest ecosystems, which make an important contribution to the global carbon cycle (Gower, 2003), are relatively more uncertain compared to ecosystems, such as the investigated grassland, whose R_{eco} can be better approximated with a single driving temperature (soil temperature in this case – see Figs. 5-6 and Table 1).

The approach applied within the context of eddy covariance CO₂ flux partitioning of minimizing the bias by choosing a driving temperature weighted between soil and air temperature with the weight determined by maximization of the nighttime R^2 , was shown to not necessarily minimize the bias between simulated and measured daytime R_{eco} (Figs. 5-6 and Table 1). We thus reinforce the recommendation by Lasslop et al. (2012) that it is important to quantify and report the uncertainty resulting from the choice of the driving temperature. For the FLUXNET 2015 data collection, processing has already gone into the direction of producing multiple GPP and R_{eco} estimates using both the Reichstein et al. (2005) and Lasslop et al. (2010) algorithms and we advocate this approach being extended to include the choice of the driving temperature. Eventually, FLUXNET data products will need to become multi-model ensembles, similar to current practise in the climate modelling community, so that the inherent systematic uncertainties in these products can be accounted for by users.

The bias could be avoided, or at least minimized, by adopting a dual-source respiration model, which would explicitly represent the major respiration sources and their temperature dependencies. Previous experience with eddy covariance CO₂ flux data (e.g. Reichstein et al., 2005), however, has shown that already a single-source model is often over-parametrized, suggesting that an adoption of Eq. (1) with four free parameters is unlikely to be successful in most cases. A notable exception may be systems that exhibit high temporal dynamics in above-ground biomass and thus respiration, which allows disentangling the above- and below-ground contributions by scaling the former with the leaf area index, as done for a temperate grassland by Wohlfahrt et al. (2005a). Ultimately, a better understanding of R_{eco} , and thus a reduced uncertainty of inferred GPP, is likely to be achieved only by separate measurements of the ecosystem respiration components (e.g. Maseyk et al., 2008), in particular the soil component, which is most amendable to direct (automated) measurements. In addition, ongoing developments of alternative approaches of estimating GPP and R_{eco} (e.g. Asaf et al., 2013; Hilker et al., 2014; Sulman et al., 2016; Wehr et al., 2016; Yang et al., 2015), need to be continued in order to be able to put the uncertainty of CO₂ flux partitioning into perspective.

Finally, we would like to reiterate (Wehr et al., 2016; Wohlfahrt et al., 2005b; Wohlfahrt and Gu, 2015) that true daytime R_{eco} is likely to be lower, at the same temperature, than nighttime R_{eco} due to reductions in leaf mitochondrial respiration during day light (the so-called Kok-effect; Heskell et al., 2013). While this did not play a role for our R_{eco} measurements, which were made with opaque chambers and darkened plants long enough to reverse the light-induced reduction of leaf respiration, for eddy covariance flux measurements, the Kok-effect must be expected to reduce daytime compared to nighttime R_{eco} , thus potentially offsetting the underestimation of daytime R_{eco} when soil temperature is chosen as the driving temperature (Fig. 1). Given the complexity of the involved processes and our poor understanding of these, we are though presently unable quantify to what degree such compensating effects may occur.

Acknowledgements

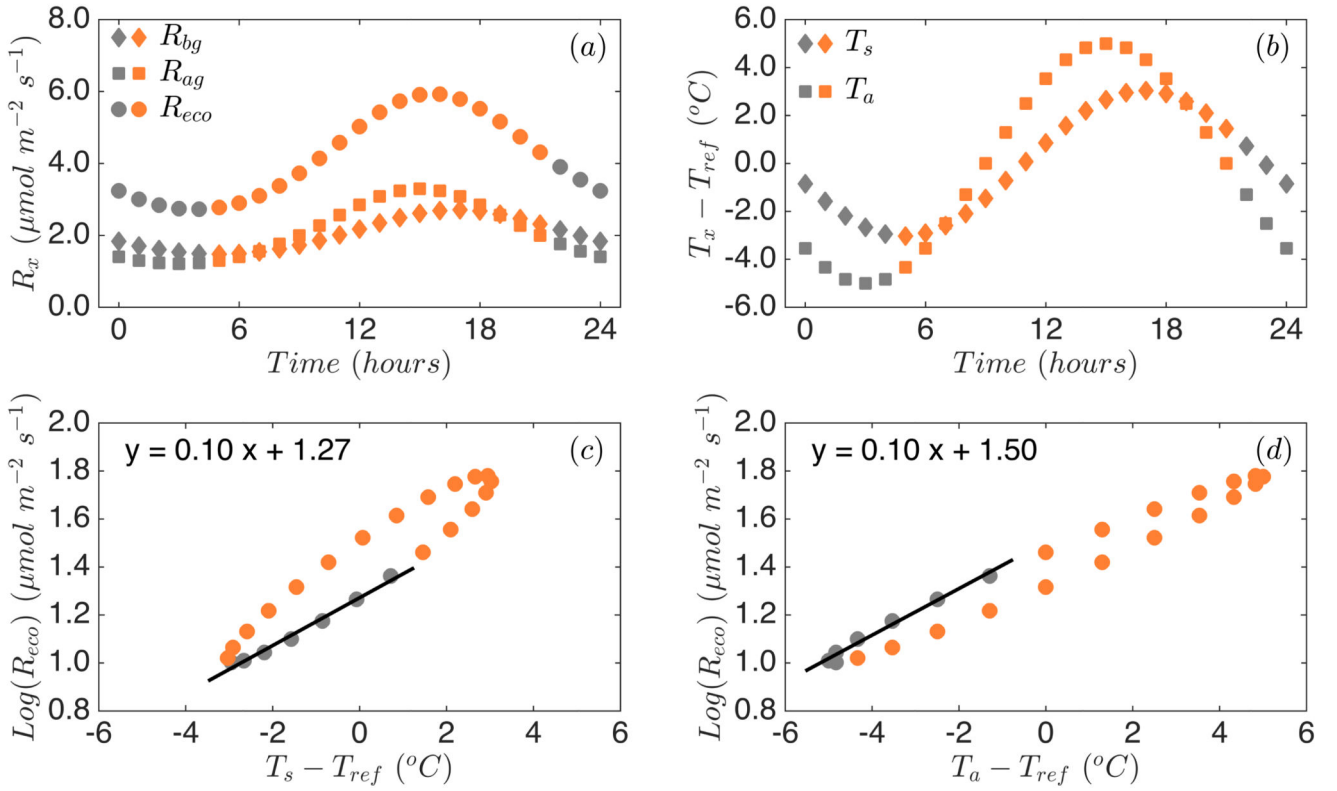
This study was financially supported by the Austrian National Science Fund under contracts P26425 and P27176.

References

- Asaf D, et al. Ecosystem photosynthesis inferred from measurements of carbonyl sulphide flux. *Nature Geoscience*. 2013; 6:186–190.
- Aubinet M. Eddy covariance CO₂ flux measurements in nocturnal conditions: An analysis of the problem. *Ecol Appl*. 2008; 18(6):1368–1378. [PubMed: 18767616]
- Bahn M, Schmitt M, Siegwolf R, Richter A, Brüggemann N. Does photosynthesis affect grassland soil-respired CO₂ and its carbon isotope composition on a diurnal timescale? *New Phytol*. 2009; 182(2):451–460. [PubMed: 19220762]
- Baldocchi D, Sturtevant C, Contributors F. Does day and night sampling reduce spurious correlation between canopy photosynthesis and ecosystem respiration? *Agric For Meteorol*. 2015; 207(0):117–126.
- Bowling DR, Tans PP, Monson RK. Partitioning net ecosystem carbon exchange with isotopic fluxes of CO₂. *Global Change Biol*. 2001; 7(2):127–145.
- Brændholt A, Steenberg Larsen K, Ibrom A, Pilegaard K. Overestimation of closed chamber soil CO₂ effluxes at low atmospheric turbulence. *Biogeosciences Discuss*. 2016

- Campbell, GS., Norman, JM. An Introduction to Environmental Biophysics. Springer; New York: 1998. p. 286
- Chapin FS, et al. Reconciling Carbon-cycle Concepts, Terminology, and Methods. *Ecosystems*. 2006; 9(7):1041–1050.
- Commane R, et al. Seasonal fluxes of carbonyl sulfide in a midlatitude forest. *Proceedings of the National Academy of Sciences*. 2015; 112(46):14162–7.
- Davidson EA, Richardson AD, Savage KE, Hollinger DY. A distinct seasonal pattern of the ratio of soil respiration to total ecosystem respiration in a spruce-dominated forest. *Global Change Biol*. 2006; 12(2):230–239.
- Galvagno M, et al. Phenology and carbon dioxide source/sink strength of a subalpine grassland in response to an exceptionally short snow season. *Environ Res Lett*. 2013; 8(2)
- Gower ST. Patterns and mechanisms of the forest carbon cycle. *Annual Review of Environment and Resources*. 2003; 28(1):169–204.
- Gu L, et al. Objective threshold determination for nighttime eddy flux filtering. *Agric For Meteorol*. 2005; 128(3–4):179–197.
- Ham, JM. Useful equations and tables in micrometeorology. *Micrometeorology in Agricultural Systems*. Hatfield, JL.Baker, JM., Viney, MK., editors. American Society of Agronomy Inc.; Crop Science Society of America Inc.; Soil Science Society of America Inc; Madison, Wisconsin, USA: 2005. p. 533-560.
- Heinemeyer A, Gornall J, Baxter R, Huntley B, Ineson P. Evaluating the carbon balance estimate from an automated ground-level flux chamber system in artificial grass mesocosms. *Ecology and Evolution*. 2013; 3(15):4998–5010. [PubMed: 24455131]
- Heskel MA, Atkin OK, Turnbull MH, Griffin KL. Bringing the Kok effect to light: A review on the integration of daytime respiration and net ecosystem exchange. *Ecosphere*. 2013; 4(8) art98.
- Hilker T, et al. Potentials and limitations for estimating daytime ecosystem respiration by combining tower-based remote sensing and carbon flux measurements. *Remote Sens Environ*. 2014; 150(0): 44–52.
- Janssens IA, et al. Productivity overshadows temperature in determining soil and ecosystem respiration across European forests. *Global Change Biol*. 2001; 7(3):269–278.
- Lasslop G, et al. On the choice of the driving temperature for eddy-covariance carbon dioxide flux partitioning. *Biogeosciences*. 2012; 9(12):5243–5259.
- Lasslop G, et al. Separation of net ecosystem exchange into assimilation and respiration using a light response curve approach: critical issues and global evaluation. *Global Change Biol*. 2010; 16(1): 187–208.
- Lloyd J, Taylor JA. On the Temperature Dependence of Soil Respiration. *Functional Ecology*. 1994; 8(3):315–323.
- Maseyk K, Grünzweig JM, Rotenberg E, Yakir D. Respiration acclimation contributes to high carbon-use efficiency in a seasonally dry pine forest. *Global Change Biol*. 2008; 14(7):1553–1567.
- Ogée J, et al. Partitioning net ecosystem carbon exchange into net assimilation and respiration using ¹³CO₂ measurements: A cost-effective sampling strategy. *Global Biogeochemical Cycles*. 2003; 17(2):1070.
- Papale D, et al. Towards a standardized processing of Net Ecosystem Exchange measured with eddy covariance technique: algorithms and uncertainty estimation. *Biogeosciences*. 2006; 3(4):571–583.
- Parazoo NC, et al. Terrestrial gross primary production inferred from satellite fluorescence and vegetation models. *Global Change Biol*. 2014; 20(10):3103–3121.
- Reichstein M, et al. On the separation of net ecosystem exchange into assimilation and ecosystem respiration: review and improved algorithm. *Global Change Biol*. 2005; 11(9):1424–1439.
- Scanlon TM, Sahu P. On the correlation structure of water vapor and carbon dioxide in the atmospheric surface layer: A basis for flux partitioning. *Water Resour Res*. 2008; 44(10)
- Speckman HN, et al. Forest ecosystem respiration estimated from eddy covariance and chamber measurements under high turbulence and substantial tree mortality from bark beetles. *Global Change Biol*. 2015; 21(2):708–721.

- Sulman BN, Roman DT, Scanlon TM, Wang L, Novick KA. Comparing methods for partitioning a decade of carbon dioxide and water vapor fluxes in a temperate forest. *Agric For Meteorol.* 2016; 226-227:229–245.
- Tramontana G, et al. Predicting carbon dioxide and energy fluxes across global FLUXNET sites with regression algorithms. *Biogeosciences.* 2016; 13(14):4291–4313.
- van Gorsel E, et al. Application of an alternative method to derive reliable estimates of nighttime respiration from eddy covariance measurements in moderately complex topography. *Agric For Meteorol.* 2008; 148(6–7):1174–1180.
- van Gorsel E, Leuning R, Cleugh HA, Keith H, Suni T. Nocturnal carbon efflux: reconciliation of eddy covariance and chamber measurements using an alternative to the u^* -threshold filtering technique. *Tellus B.* 2007; 59(3):397–403.
- Vickers D, Thomas CK, Martin JG, Law B. Self-correlation between assimilation and respiration resulting from flux partitioning of eddy-covariance CO_2 fluxes. *Agric For Meteorol.* 2009; 149(9): 1552–1555.
- Wehr R, et al. Seasonality of temperate forest photosynthesis and daytime respiration. *Nature.* 2016; 534(7609):680–3. [PubMed: 27357794]
- Wehr R, Saleska SR. An improved isotopic method for partitioning net ecosystem–atmosphere CO_2 exchange. *Agric For Meteorol.* 2015; 214–215:515–531.
- Wohlfahrt G, et al. Quantifying nighttime ecosystem respiration of a meadow using eddy covariance, chambers and modelling. *Agric For Meteorol.* 2005a; 128(3–4):141–162.
- Wohlfahrt G, Bahn M, Haslwanter A, Newesely C, Cernusca A. Estimation of daytime ecosystem respiration to determine gross primary production of a mountain meadow. *Agric For Meteorol.* 2005b; 130(1–2):13–25.
- Wohlfahrt G, Gu L. The many meanings of gross photosynthesis and their implication for photosynthesis research from leaf to globe. *Plant Cell Environ.* 2015; 38(12):2500–2507. [PubMed: 25988305]
- Yang X, et al. Solar-induced chlorophyll fluorescence that correlates with canopy photosynthesis on diurnal and seasonal scales in a temperate deciduous forest. *Geophys Res Lett.* 2015; 42(8):2977–2987.

**Figure 1.**

Simulated (a) below-ground, above-ground and ecosystem respiration, (b) soil and air temperature, and hysteresis relationships between ecosystem respiration and (c) soil and (d) air temperature. Orange symbols refer to daytime, grey symbols to nighttime periods. Lines in lower panels represent linear regressions to nighttime data, with the regression coefficients indicated. Model parameters were set to: $R_{ag}@T_{ref} = R_{bg}@T_{ref} = 2 \mu\text{mol m}^{-2} \text{s}^{-1}$; $E_{o_ag} = E_{o_bg} = 0.1 \text{ K}^{-1}$; $T_{avg} = 293 \text{ K}$; $A_o = 5 \text{ K}$; $z = 0.05 \text{ m}$; $D = 0.1 \text{ m}$.

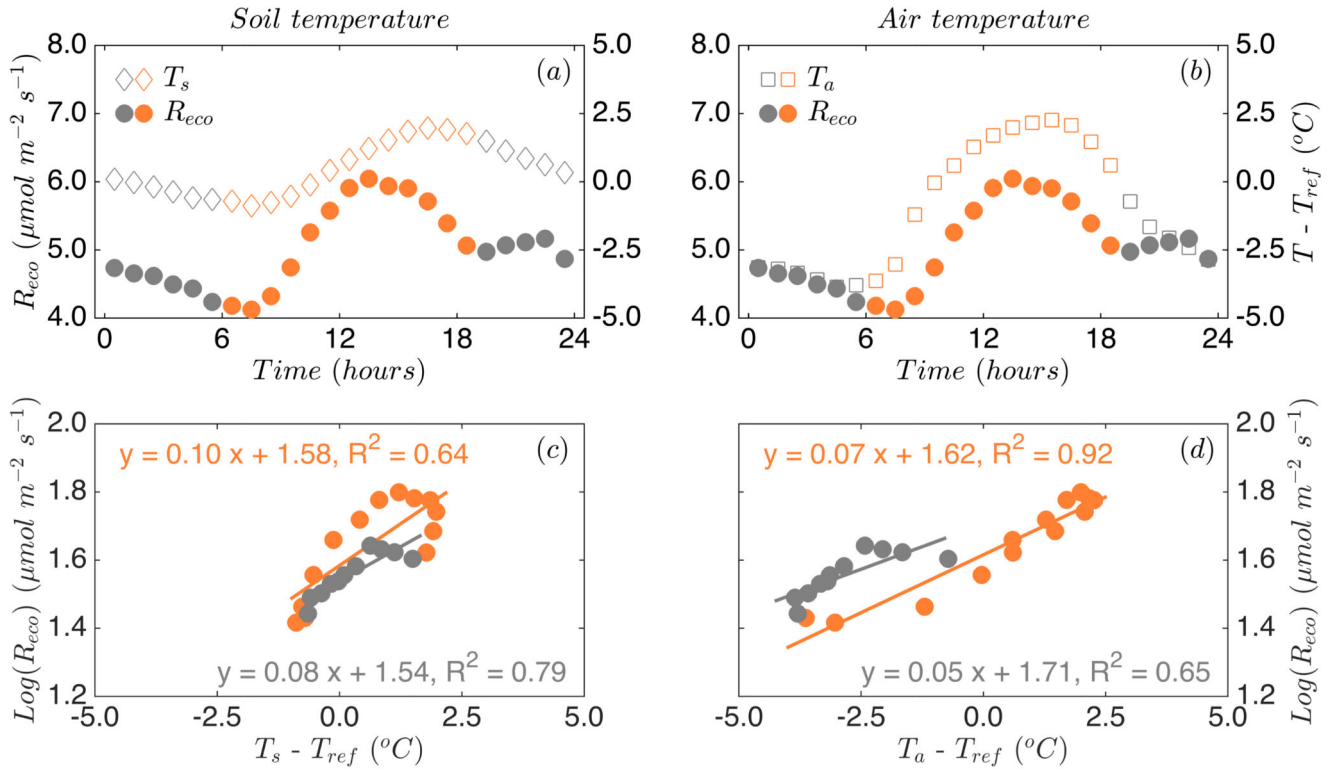


Figure 2.

Bin-averaged diurnal courses of soil (a) and air (b) temperature and ecosystem respiration (a, b) and hysteresis relationship between ecosystem respiration and soil (c) and air (d) temperature. Orange symbols refer to daytime, grey symbols to nighttime periods. Lines in lower panels represent linear regressions to day (orange lines) and nighttime (grey lines) data, with the regression coefficients indicated.

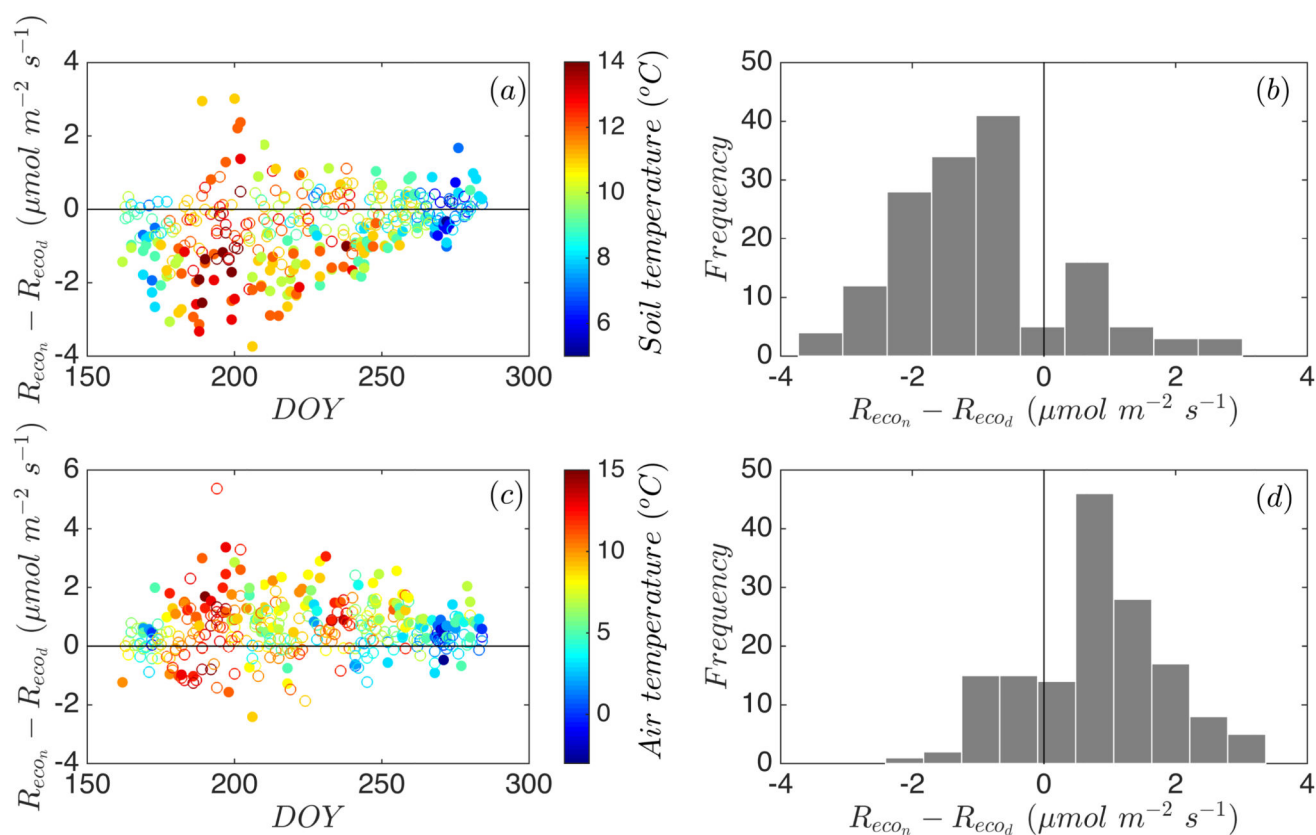


Figure 3.

Differences between nighttime and daytime R_{eco} at same temperature (within one degree bins) based on soil (a, b) and air (c, d) temperature. Closed symbols in (a) and (c) indicate significant differences at $p < 0.05$.

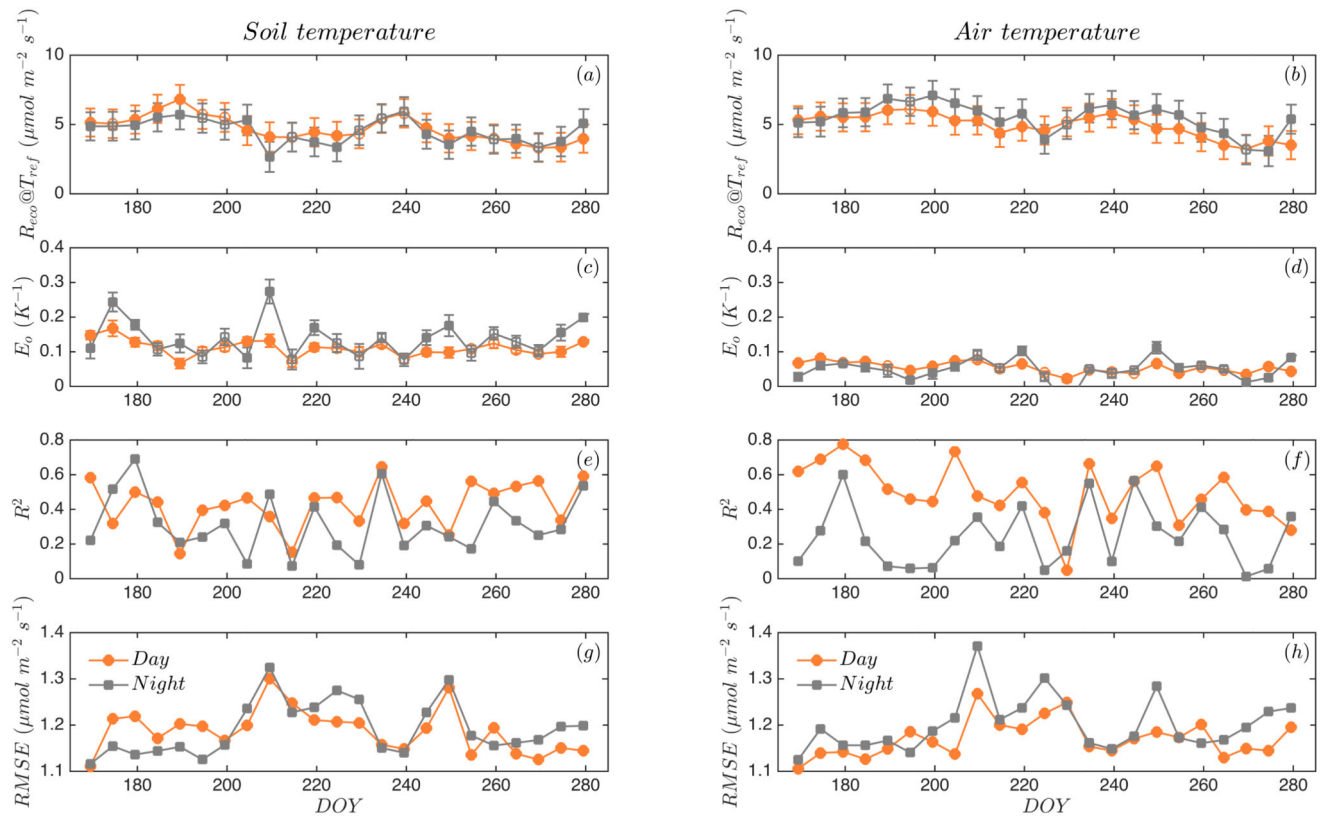


Figure 4.

Seasonal results of the calibration of the daytime (orange symbols and lines) and nighttime (grey symbols and lines) temperature response of ecosystem respiration (Eq. 4) using soil (left panels) and air temperature (right panels). Shown are the ecosystem respiration at the reference temperature (a, b; inclusive of one standard deviation), the temperature sensitivity parameter (c, d; inclusive of one standard deviation), the coefficient of determination (e, f), and the root mean squared error (g, h). Each data point refers to a 15-day period with a 5-day moving time window. Closed symbols in panels a-d indicate significant differences ($p < 0.05$) between day and night.

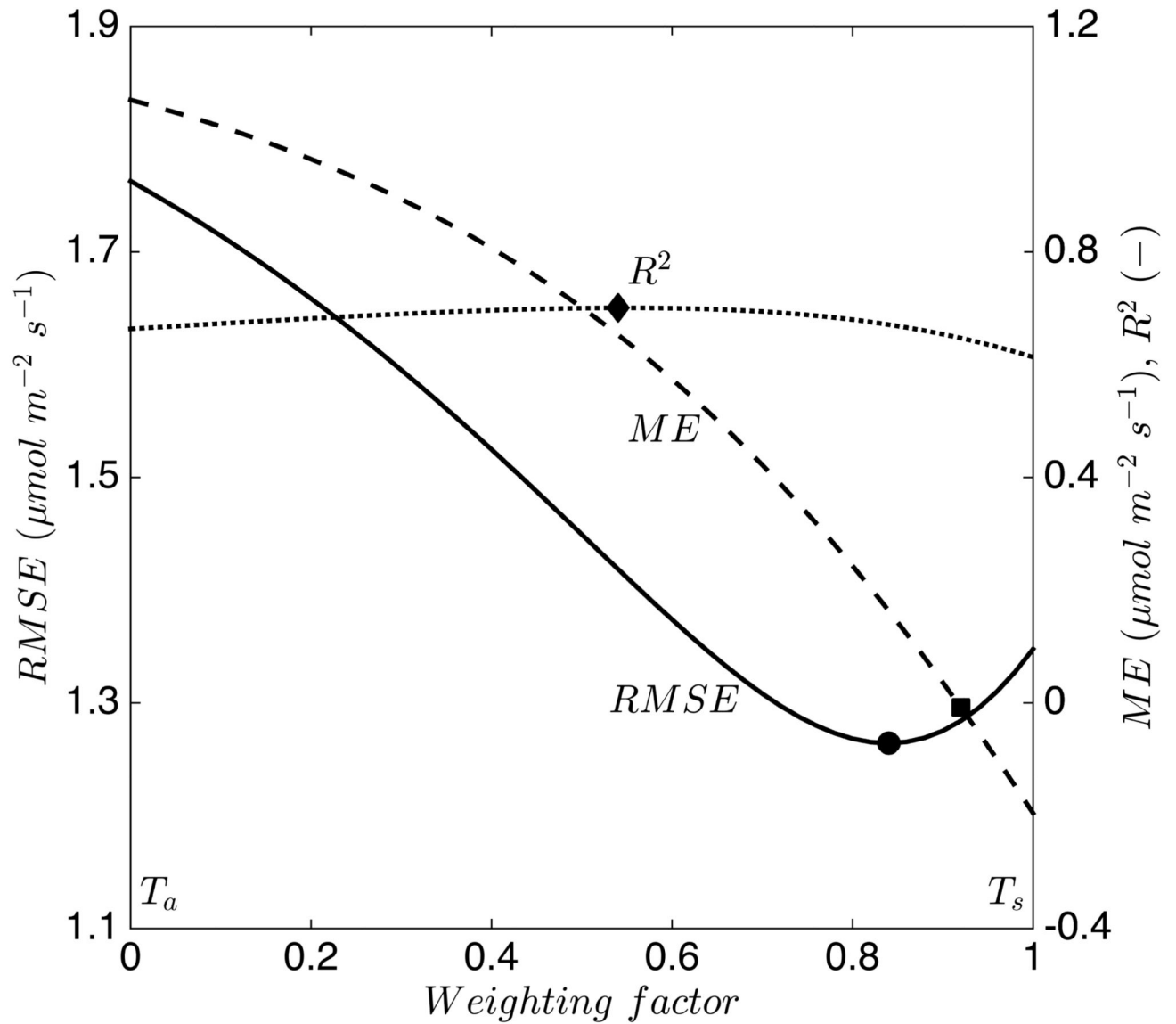
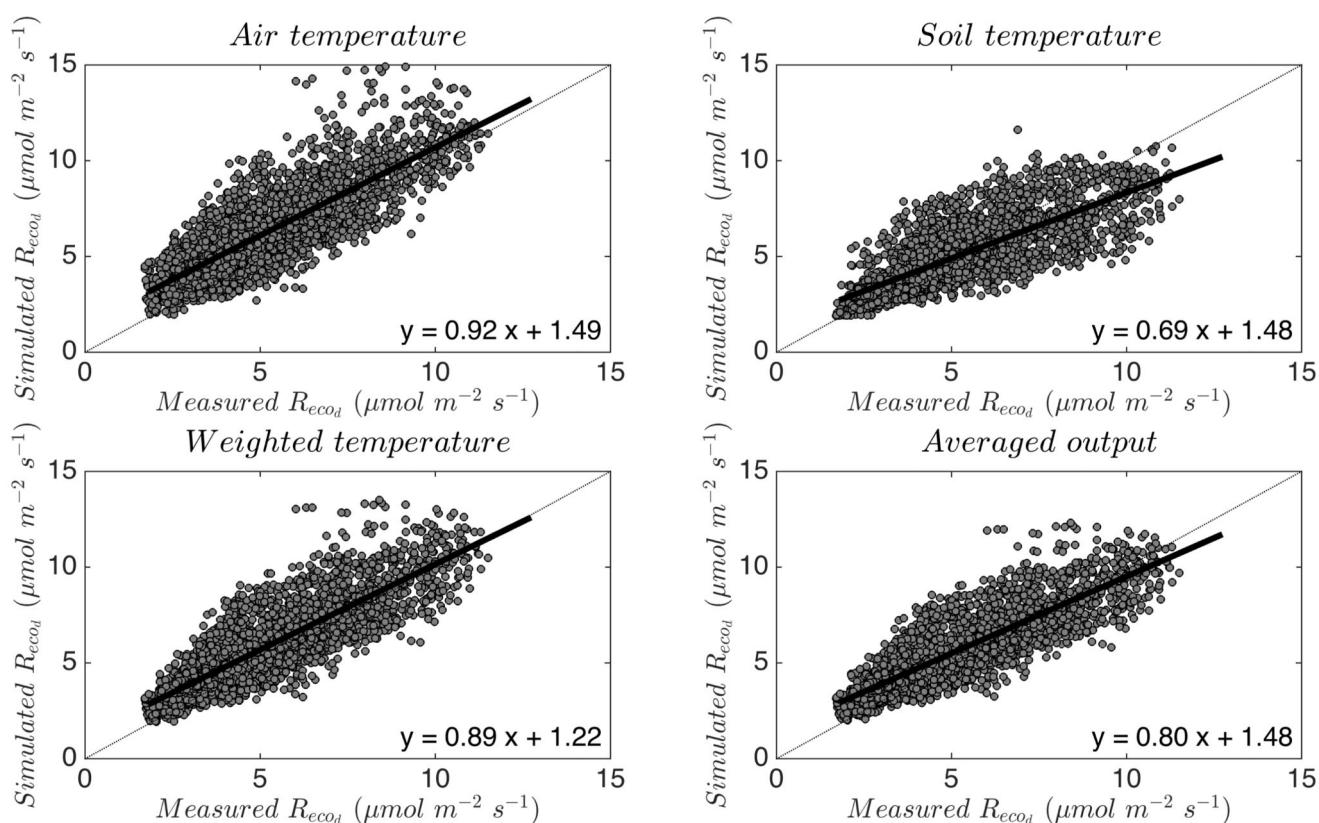


Figure 5.

Effects of changing the weighting factor (w) between soil and air temperature ($T_s w + T_a (1-w)$) on the fraction of explained variability (R^2) in nighttime R_{eco} , and the root mean square error (RMSE) and mean error (ME) between the measured and estimated daytime R_{eco} . The maximum R^2 and minimum RMSE and ME are indicated by symbols.

**Figure 6.**

Comparison between measured daytime ecosystem respiration and ecosystem respiration simulated based on soil and air temperature, a weighted average temperature ($0.54 T_s + 0.46 T_a$ – see text for details) and by averaging the ecosystem respiration simulated with air and soil temperature. Solid lines represent linear regressions, for which the coefficients are indicated the lower right corners of each panel.

Table 1

Statistical comparison between simulated, parameterised with nighttime data, and measured daytime ecosystem respiration (coefficient of determination – R^2 ; modelling efficiency – MEF; root mean squared error – RMSE ($\mu\text{mol m}^{-2} \text{s}^{-1}$); mean error – ME ($\mu\text{mol m}^{-2} \text{s}^{-1}$)). Values represent means \pm one standard deviation derived from 1000 bootstrapping loops. All differences between the four approaches are significant at $p < 0.05$.

	Soil temperature	Air temperature	Weighted average temperature	Averaged output
R^2	0.61 ± 0.00	0.66 ± 0.00	0.70 ± 0.00	0.70 ± 0.00
MEF	0.60 ± 0.00	0.31 ± 0.04	0.55 ± 0.02	0.64 ± 0.01
RMSE	1.15 ± 0.02	1.39 ± 0.03	1.24 ± 0.02	1.12 ± 0.02
ME	0.20 ± 0.03	-1.07 ± 0.05	-0.65 ± 0.04	-0.44 ± 0.04